ACS MATERIALS LETTERS

www.acsmaterialsletters.org

LETTER

Multistage Transdermal Nitric Oxide Delivery System for the Efficient Treatment of Androgenic Alopecia

Hui Xing,[#] Xinlin Jiang,[#] Ziyi Zhao, Yuhui Yang, Zhen Wang, Yang Yi, Guodong Sun, Shixin Liu,* and Dong Ma*

Cite This: *ACS Materials Lett.* 2024, 6, 5354−5362

Read Online

ACCESS | Metrics & More | Article Recommendations | Supporting Information

ABSTRACT: **Androgenic alopecia (AGA) is a prevalent progressive hair loss condition. The main therapeutic drug, minoxidil, is limited by its poor efficacy and side effects such as contact dermatitis and hypertrichosis. Nitric oxide (NO), an endothelial-derived relaxing factor, promotes angiogenesis and accelerates blood flow, enhancing nutrient supply similar to minoxidil. Accordingly, we utilized a poly(vinyl alcohol) film (PVA) loaded with hyaluronic acid (HA) liposomes to construct a multistage transdermal NO delivery system (PVA@HL/NONOate) for the treatment of AGA. The HA liposomes provided efficient NO loading and extended release, while the PVA film improved skin penetration and sustained NO release, increasing NO bioavailability. Low-concentration NO effectively enhanced hair follicle vitality and repaired blood vessels. Mechanistically, low-concentration NO could treat AGA mainly by regulating the HIF-1 signaling pathway to promote angiogenesis, reducing inflammation by downregulating the expression of TNFRSF9 and IL-6, repairing hair follicles by downregulating the expression of genes in the CXCL5-IL-17 inflammatory axis.**

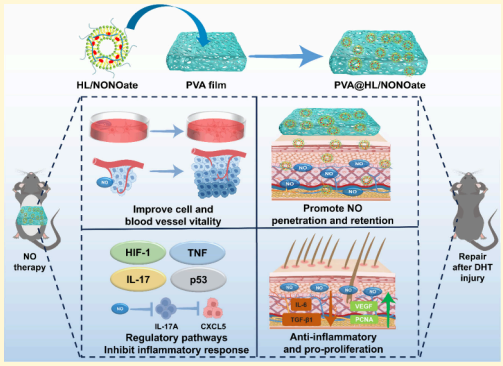

Androgenic alopecia (AGA) is a globally common disease that causes significant distress to affected individuals.[1] Minoxidil, the first FDA-approved drug for AGA, is a vasodilator and potassium channel opener, which treats hair loss by increasing blood flow and increasing nutrient supply to hair follicles. However, commercial minoxidil preparations contain cytotoxic ingredients such as ethanol and propylene glycol, which lead to side effects like scalp dryness, irritation, and itching in long-term use.[2] Thus, new treatment strategies are urgently needed. Gas therapy involves the exogenous administration of gas molecules with specific therapeutic effects, which not only avoids drug resistance but also increases the sensitivity of resistant cells to drugs, presenting a promising "green" therapeutic strategy.[3] Among various gas molecules, nitric oxide (NO) is an endogenous relaxing factor involved in physiological processes such as vasodilation, proliferation, apoptosis, and gene transcription regulation.[4] Studies have shown that low-concentration NO have great potential in enhancing cell viability, promoting vasodilation, and accelerating blood circulation, which is similar to the mechanism by which minoxidil treats AGA.[5,6] However, the mechanism of NO in treating AGA has not been well understood. Meanwhile, the stratum corneum of the skin serves as the first barrier, preventing NO from achieving therapeutic purposes through transdermal delivery.

Liposomes, due to their prominent epidermis-penetration capacity, high encapsulation efficiency and good stability, have gained significant attention as nanodrug delivery systems. For instance, Yoshikawa et al. found that liposomes could maintain the long term stability of NO donors, rapidly and continuously accumulate in tumor tissues, and enhance the enhanced permeability and retention effect.[7] Hyaluronic acid (HA), as an excellent transdermal promoting agent, can cause skin tissue to swell and form molecular transport channels due to its abundant hydroxyl groups in main chains. Its hydrophobic groups can disrupt the skin barrier through lipid interactions and enhance penetration of transdermal systems.[8] For example, Zhang et al. developed HA-modified liposomes (HA-UP-LPs) and discovered that, in comparison to conventional cationic

Received: September 16, 2024
Revised: November 3, 2024
Accepted: November 4, 2024

https://doi.org/10.1021/acsmaterialslett.4c01891
ACS Materials Lett. 2024, 6, 5354−5362

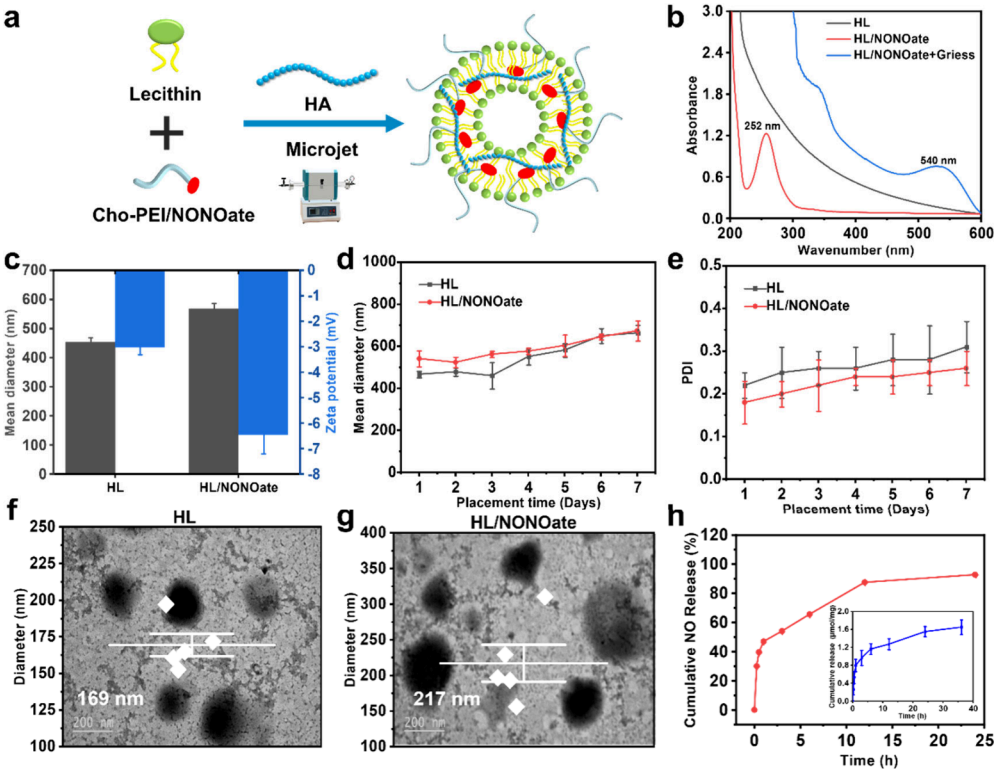

Figure 1. (a) Diagrammatic illustration of the primary transdermal delivery system. (b) UV spectra of HL, HL/NONOate, and HL/NONOate+Griess reagent. (c) Average particle diameter and zeta potential of nanoparticles. (d) Stability of HL and HL/NONOate over 7 days. (e) Changes in the PDI of HL, HL/NONOate over 7 days. TEM images of HL (f) and HL/NONOate (g) (n = 5), scale bar = 200 nm. (h) NO content and release characteristics in the HL/NONOate.

liposomes, HA-UP-LPs exhibited enhanced potential and promising application prospects in targeted transdermal drug delivery.[9]

Poly(vinyl alcohol) (PVA) is widely used as a biomaterial due to its good biocompatibility and degradability. The unique properties of PVA films allow for drug loading into the matrix through the regulation of porous structures, achieving sustained drug release and skin penetration. Suitable drug-release forms can maintain constant drug concentration for a long period to avoid cytotoxicity from burst release, presenting broad prospects in drug delivery fields.[10] In order to create a transdermal delivery method for the treatment of melanoma, Ni et al. recently combined multistage targeted liposomes into a hydrogel matrix, exhibiting high penetration, stability, and permeability.[11] Inspired by the multistage transdermal system, we aimed to address issues including NO loading, unstable release, and poor transdermal delivery efficiency by constructing a multistage gas delivery vehicle combining the advantages of liposomes, HA, PVA, and NO gas therapy for treating AGA.

We conceptualized hair follicles of AGA patients as seeds, PVA films as soil, and NO as fertilizer, aiming to achieve therapeutic effects by continuously supplying nutrients to damaged hair follicles through highly efficient multistage delivery of NO. Based on preliminary research, we selected small molecular weight polyethylenimine-modified cholesterol esters as NO donors. These donors were then combined with lecithin and HA molecules to prepare HL/NONOate utilizing a one-step procedure. HL/NONOate was then seeded into a PVA film-based secondary delivery vehicle, resulting in a multistage transdermal NO delivery system with efficient penetration and therapeutic functions (PVA@HL/NONOate). First, we explored the preparation process of HL/NONOate through various methods and conducted a detailed investigation of the stability and NO release performance of this primary system. Next, cell experiments were carried out to investigate the impact of NO on the proliferation and migration viability of human dermal papilla cells (HDPCs) and human umbilical vein endothelial cells (HUVECs). RNA sequencing was used to identify potential target genes and regulatory pathways for NO, summarizing the mechanisms by which low-concentration NO promote hair growth and repair damaged hair follicles. Multiple research methods were employed to investigate the film-forming properties of PVA@HL/NONOate carriers and analyze the dynamics of NO penetration in the skin. To evaluate the therapeutic effects of NO, an AGA mouse model was established, employing various research parameters, and a thorough analysis of biosafety was conducted.

As shown in Figure 1a, a primary NO transdermal delivery carrier was constructed by incorporating NO donors into the liposome structure, resulting in a NO carrier with a small particle size, high loading capacity, and extended release period. As shown in Figure S1a, the peaks of methylene groups in the main and side chains of PEI appear between 2.5 and 3 ppm, with the allylic position peaks of Cho between 5.0 and 5.5 ppm, and the peaks of Cho methyl and methylene groups between 0.5 and 0.9 ppm, confirming the successful synthesis of Cho-PEI. As shown in Figure S1b, Cho exhibits a distinct peak at 1720 cm^{-1} corresponding to the acyl chloride group. After reacting with PEI, a peak at 1680 cm^{-1} due to the −CO-NH- stretching vibration appears in Cho-PEI, indicating the transformation of the acyl chloride to an amide group and

https://doi.org/10.1021/acsmaterialslett.4c01891
ACS Materials Lett. 2024, 6, 5354−5362

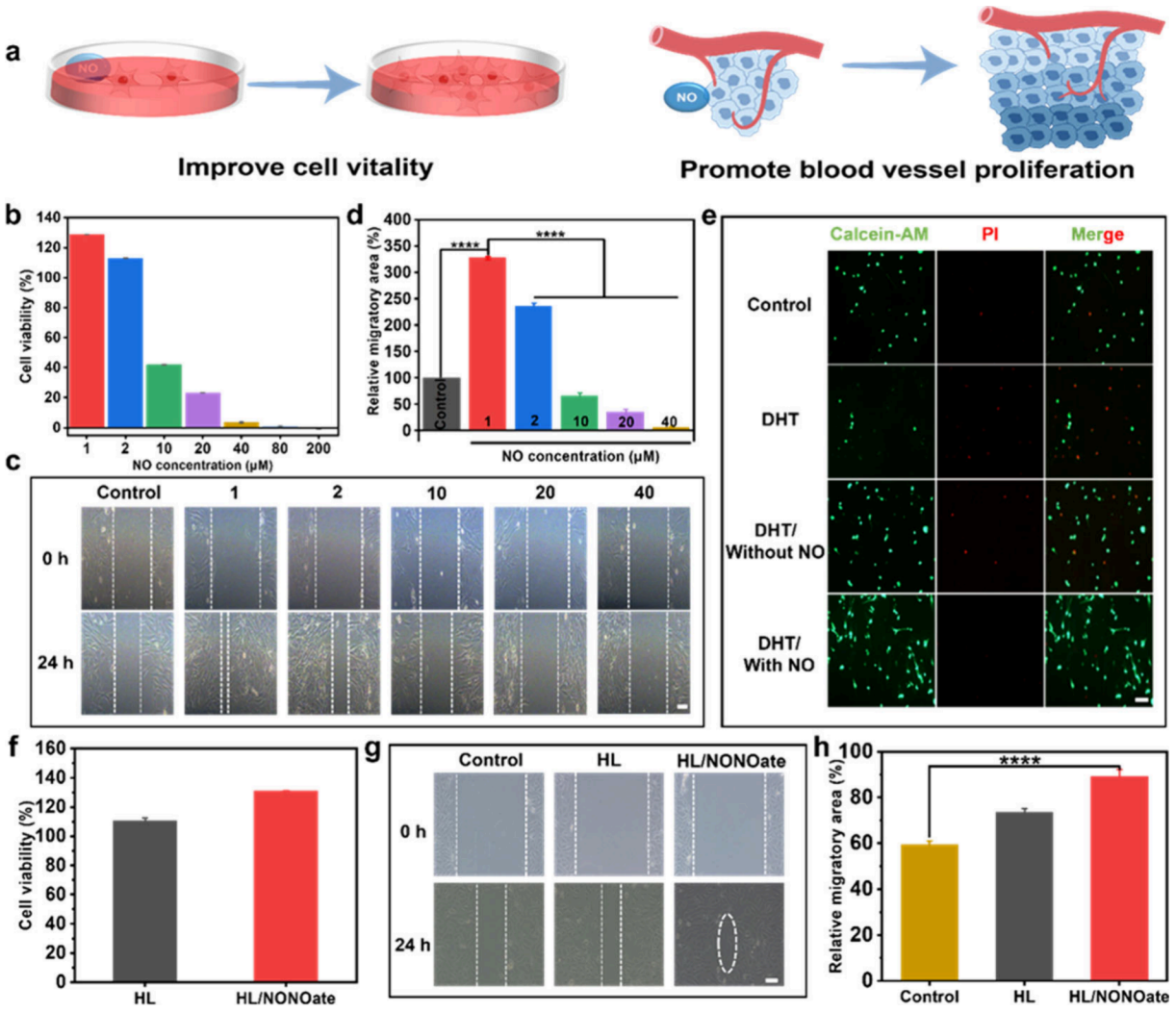

Figure 2. (a) Diagram illustrating NO promotion of cell proliferation and angiogenesis. (b) Proliferation rates of HDPCs after treatments with different concentrations of NO (1, 2, 10, 20, 40, 80, and 200 μM) (n = 3). (c) Migration images of HDPCs after treatments with different concentrations of NO (1, 2, 10, 20, and 40 μM), scale bar = 100 μm. (d) A quantitative assessment of the relative regions of migration from (c). (e) Live/dead staining images of HDPCs damaged by DHT treated with 1 μM NO. (f) Effect of 1 μM NO on HUVECs proliferation (n = 3). (g) Effect of 1 μM NO on HUVECs migration, scale bar = 100 μm. (h) A quantitative assessment of the relative regions of migration from (g). *p < 0.05, **p < 0.01, ***p < 0.001 and ****p < 0.0001.

further confirming the successful synthesis of Cho-PEI. Compared to Cho-PEI, Cho-PEI/NONOate shows a characteristic absorption peak of the NONOate group at 1550 cm^{-1}.[6] As shown in Figure 1b, HL/NONOate exhibited a characteristic UV absorption peak of the NONOate group at 252 nm, further confirming the successful embedding of NO. As shown in Figure 1c, indicate that both nanocarriers have hydrated particle sizes below 600 nm. Transmission electron microscopy (TEM) analysis, depicted in Figure 1f, g, revealed that both nanocarriers possess spherical vesicular structures with similar shapes. After drying, the size remained stable at approximately 200 nm, indicating that the formulation meets the basic requirements for skin penetration.[12] Maintaining a stable liposomal complex structure is crucial for transdermal drug delivery and therapeutic therapy.[13] The PDI represents the distribution of particle sizes in a population. It ranges from 0 to 1, with smaller values indicating a more concentrated particle size distribution, which is beneficial for transdermal delivery. If the PDI value approaches 1, it suggests a wide size distribution. Even if the average particle size meets the requirements, a broad size distribution indicates the presence of large particles, which may hinder transdermal penetration.[14] As shown in Figure 1d, e, there was a slight increase in particle size for both nanocarriers, but the changes were minimal, and the particle size and PDI remained relatively consistent over the seven-day period, the uniform distribution observed further supports the formulation's stability. Overall, the delivery vectors prepared using this technique exhibit small particle sizes and high stability, effectively facilitating the delivery of NO active molecules.

As NO acts as a "green" molecule loaded into liposomes for therapeutic effects, it is important to assess how well NO loads into HL/NONOate and how it releases. To hasten the release of NO, a pH 4.0 buffer was added, in accordance with the NO release properties of the N-diazeniumdiolate (NONOate). Using the standard curve, the final loading level of NO in Cho-PEI/NONOate was determined to be 1.47 μmol/mg. Additionally, as shown in Figure 1h, the release rate of NO from HL/NONOate was quite apparent in the early stages, with about 65% of NO released within 5 h. The release rate

https://doi.org/10.1021/acsmaterialslett.4c01891
ACS Materials Lett. 2024, 6, 5354−5362

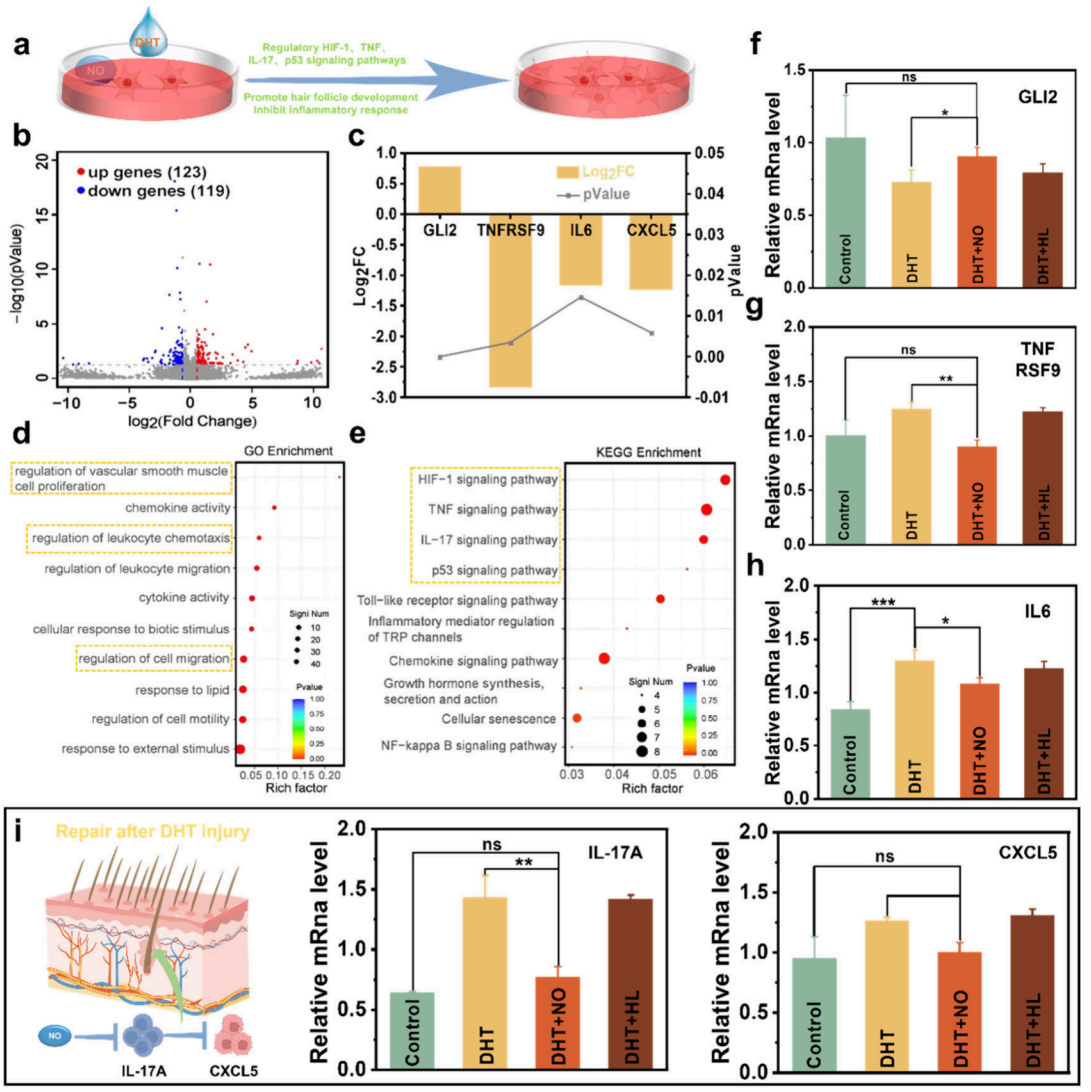

Figure 3. (a) Diagram illustrating the pathways and mechanisms of NO treatment in damaged HDPCs. (b) Differential gene expression analysis in HDPCs with and without NO treatment. (c) Representative sequencing analysis of genes related to hair follicles. (d) GO analysis of differentially expressed genes in HDPCs damaged by DHT and treated with NO. (e) KEGG analysis of differentially expressed genes in HDPCs damaged by DHT and treated with NO. (f) Sequencing analysis of the expression of the GLI2 gene in hair follicles (n = 3). (g) Sequencing analysis of the expression of the TNFRSF9 gene in hair follicles (n = 3). (h) Sequencing analysis of the expression of the IL6 gene in hair follicles (n = 3). (i) NO promotes the repair of damaged hair follicles through the IL-17 signaling pathway by controlling the CXCL5-IL-17 inflammatory axis (n = 3). *p < 0.05, **p < 0.01, ***p < 0.001 and ****p < 0.0001.

then fell, reaching a steady, slow-release condition. After 12 h, the NO release approached 90%, and by 24 h, the NO release was essentially complete. The sustained NO release characteristics of HL/NONOate provide a crucial material foundation for achieving effective transdermal delivery and maintaining long-term therapeutic effects.

The direct causes to AGA including dermal papilla damage and vascular degeneration of hair follicles have been extensively studied.[15,16] As shown in Figure 2a, effects of NO on the proliferation and migration of HDPCs and on the protection against dihydrotestosterone (DHT) damage was first explored to determine the optimal therapeutic concentration for subsequent experiments on the proliferation and migration of HUVECs to assess their effects on angiogenesis and nutrient supply. As shown in Figure 2b, different concentrations of NO had varying effects, and concentrations greater than 2 μM exhibited inhibitory effects. Innovatively, it was found that concentrations below 2 μM significantly enhanced the proliferation of HDPCs, with proliferation increases of 112.99% ± 0.1% and 128.69% ± 0.04%, respectively. These results were validated in an *in vitro* migration assay for HDPCs. As shown in Figure 2c, d, 1 μM NO significantly reduced the scratch area after 24 h compared to the other NO concentrations, achieving more than three times the effect of the control group. This confirms the advantage of NO in enhancing the vitality of hair follicle cells. As shown in Figure 2e and Figure S2a, under treatment with 1 μM NO, the cell death rate of HDPCs was significantly reduced, showing only weak red fluorescence signals, while the survival rate was significantly increased (green fluorescence signals), further proving the excellent therapeutic effects and cellular safety of low concentration NO. In response to the issue of miniaturization of hair follicle vessels and insufficient blood nutrient supply caused by AGA, we first investigated the effect of different NO concentrations on the viability of HUVECs. As shown in Figure S2b, similar to the results

https://doi.org/10.1021/acsmaterialslett.4c01891
ACS Materials Lett. 2024, 6, 5354−5362

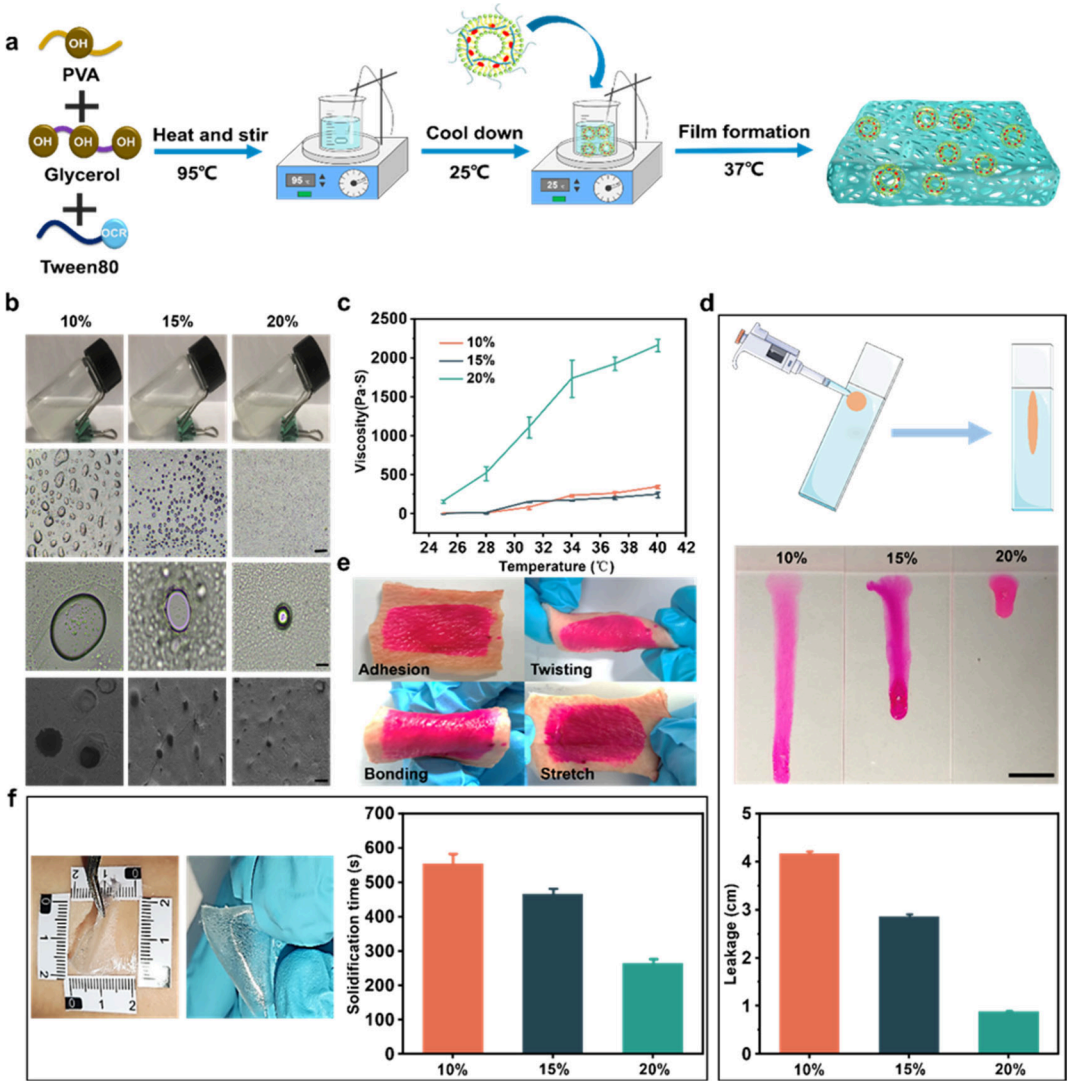

Figure 4. (a) Diagram illustrating the synthesis of PVA@HL/NONOate. (b) From top to bottom: photographs of PVA@HL/NONOate at different PVA concentrations, images of pore sizes under an optical microscope and SEM. (c) Changes in the viscosity of PVA@HL/NONOate at different PVA concentrations (n = 3). (d) Adhesion tests of PVA@HL/NONOate at different PVA concentrations (n = 3). (e) Mechanical flexibility test of PVA@HL/NONOate at a 20% PVA concentration. (f) Film-forming capability tests of PVA@HL/NONOate at various PVA concentrations (n = 3).

observed with HDPCs, NO concentrations greater than 2 μM exhibited a significant inhibitory effect, while concentrations below 2 μM demonstrated a promotive effect. Next, the effects of 1 μM NO on the *in vitro* proliferation and migration capabilities of HUVECs were explored. As shown in Figure 2f, the NO group showed a proliferation enhancement of 130.89% ± 0.4%, these experimental results were validated again in the *in vitro* migration experiment after 24 h (Figure 2g, h), thus low-concentration NO also has excellent effects on promoting vascular proliferation, providing a theoretical basis for the treatment of androgenic alopecia.

To further explore the regulatory effects of NO on related cells and understand the molecular mechanisms of NO treatment for AGA, this study utilized high-throughput sequencing technology to perform RNA sequencing on HDPCs damaged by androgens and treated with NO (Figure 3a). As shown in Figure 3b, after NO treatment, 123 genes were upregulated and 119 genes were downregulated. Among these genes, four significantly related to hair follicle growth were identified: GLI2, TNFRSF9, IL6, and CXCL5, as displayed in Figure 3c. GLI2, a gene associated with hair diseases, controls the early growth and development of hair, while the high expression of TNFRSF9, IL6, and CXCL5 indicates an increase in follicular cell inflammation, signaling the onset of the regression phase.[17,18] As illustrated in Figure 3f, g, h, the damaging effect of DHT on HDPCs was significant, with a notable upregulation of TNFRSF9 and IL6 in damaged cells compared to normal cells, whereas in the NO group, TNFRSF9 and IL6 were significantly downregulated and there was no significant difference from the Control group, demonstrating the anti-inflammatory effects of low-concentration NO on HDPCs. Compared to the DHT group, the significant upregulation of the GLI2 gene in the NO group and there was no significant difference from the Control group, confirming that low-concentration NO can treat AGA by regulating hair follicle growth genes. As shown in Figure 3e, the differentially expressed genes related to hair growth were mainly enriched in the HIF-1, TNF, IL-17, and p53 signaling pathways. The HIF-1 pathway can promote the expression of VEGF, enhancing angiogenesis, while the TNF and IL-17

https://doi.org/10.1021/acsmaterialslett.4c01891
ACS Materials Lett. 2024, 6, 5354−5362

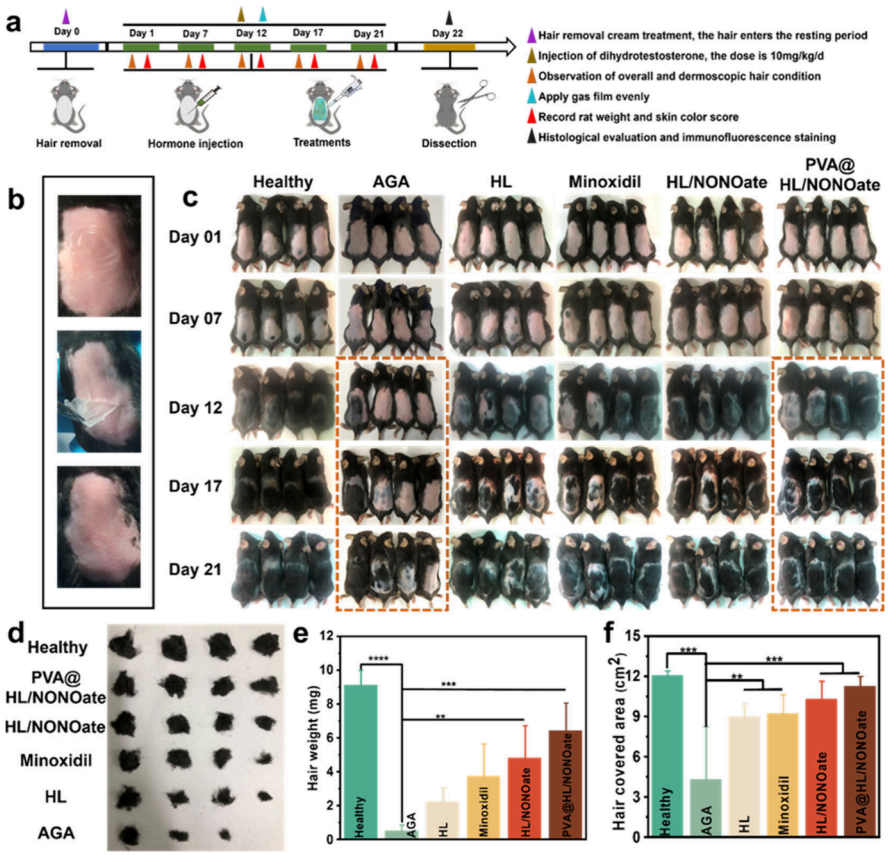

Figure 5. (a) Creation of the AGA mouse model and an outline of the treatment plan. (b) Treatment process of AGA mice with PVA@HL/NONOate. (c) Photos of mice after depilation treated with HL, Minoxidil, HL/NONOate, and PVA@HL/NONOate (n = 4). (d) Photos depicting new hair growth in mice (n = 4). (e) Weight of new hair growth in mice (n = 4). (f) Area of new hair growth in mice (n = 4). *p < 0.05, **p < 0.01, ***p < 0.001 and ****p < 0.0001.

pathways play crucial roles in follicular inflammation and immune responses, and the p53 pathway is important in regulating the hair follicle cycle.[19−21] A GO analysis was also conducted, as shown in Figure 3d, which again confirmed that low-concentration NO positively affects the treatment of AGA by regulating vascular proliferation, inhibiting inflammatory responses, and promoting cell migration. Previous studies had also found that the CXCL5-IL-17 inflammatory axis can effectively promote hair follicle stem cell differentiation, thus influencing growth and development.[20] As depicted in Figure 3i, low-concentration NO can regulate the IL-17 signaling pathway, downregulating the expression of IL-17A and CXCL5 genes to repair follicles damaged by DHT and promote their growth and development. This study, combining high-throughput sequencing technology, detailedly explored the molecular mechanisms of NO treatment for AGA, providing theoretical support for subsequent clinical applications.

This study successfully constructed a multistage transdermal delivery system PVA@HL/NONOate to enhance the transdermal effect and bioavailability of NO (Figure 4a). As shown in Figure 4b, PVA@HL/NONOate exhibits a well-defined three-dimensional porous structure, with the porosity gradually decreasing as the PVA concentration increases. This is expected to enhance the material's surface area and improve its adsorption capacity, allowing for more efficient loading of HL/NONOate. By preventing gas exchange with the external environment, this structure can further facilitate the transdermal penetration of NO.[22] As shown in Figure S3b, compared to HL/NONOate, PVA@HL/NONOate exhibited a more sustained release of NO, with a release duration of up to 30 h. This extended release ensures the continuous action of NO during subsequent animal treatment, contributing to its therapeutic effectiveness. The viscosity of the carrier solution as it changes with temperature was explored using a rheometer. It is noted that at near human body temperature, a 20% concentration displays a significant advantage, exhibiting more than eight times the viscosity of other concentrations, which suits application on the skin surface (Figure 4c). By adding rhodamine to the carrier for imaging purposes, it is observed that on pig skin, the carrier adheres well under various conditions and exhibits good mechanical flexibility (Figure 4e). As shown in Figure 4d, the 20% concentration carrier showed the best adhesion effect, with a leakage distance of only 0.87 ± 0.03 cm. Lastly, the film-forming and degradation properties of the delivery carrier were tested. As seen in Figure 4f and Figure S3a, it was observed that the carrier formed a complete porous film on the surface of human skin within 5 min, and the structure remained intact after 24 h. This indicates that the material meets the requirements for skin application, allowing it to adhere to the skin surface for an extended period, which is beneficial for sustained transdermal NO therapy.

In vitro experiments were conducted to simulate human transdermal permeation to monitor the permeation efficiency of NO in PVA@HL/NONOate through the skin (Figure S4a). As shown in Figure S4b, indicated that the cumulative permeation of NO through the skin increased over the 12-h

https://doi.org/10.1021/acsmaterialslett.4c01891
ACS Materials Lett. 2024, 6, 5354−5362

observation period for both PVA@HL/NONOate and HL/NONOate. Notably, PVA@HL/NONOate demonstrated superior NO permeation as early as 2 h, with a significantly higher cumulative permeation over 12 h compared to HL/NONOate. Furthermore, after applying PVA@HL/NONOate to the dorsal skin of live mice for 1 h, NO content was measured using immunohistochemistry. As illustrated in Figure S5, the PVA@HL/NONOate group exhibited a noticeable increase in gray scale in the mouse skin, and quantitative analysis showed that the NO content was higher compared with that in the HL/NONOate group.

To assess the clinical efficacy of NO in treating AGA, a model was established by injecting dihydrotestosterone into the back of mice every day (Figure 5a). The application of PVA@HL/NONOate, as illustrated in Figure 5b, a uniform application of 200 μL of PVA@HL/NONOate was administered daily to the dorsal region of mice. After 5 min, the formulation spontaneously formed a film, facilitating gas permeation. After 24 h, the film could be easily removed by applying pure water, leaving no residue. No adverse reactions or discomfort were observed on the mice's skin following treatment. As shown in Figure S6c, the stable body weight of mice indicated that they were in good health. In Figure 5c and Figure S7b, within the first 7 days after hair removal, no significant hair growth was observed in the dihydrotestosterone injection groups, whereas the skin color of the Healthy group began to turn gray, with visible hair growth under the skin microscope. By day 12, noticeable hair growth was observed on the back of the Healthy group, while the skin color of the treated mice turned gray, and the PVA@HL/NONOate group showed visible hair regrowth in certain areas, confirmed under the microscope. Continued treatment from day 17 to day 21 resulted in complete hair regrowth with a healthy appearance in the Healthy group, but the AGA group showed only isolated hair regrowth and minimal hair under the microscope, indicating that the AGA model remained stable over time. On day 21, the PVA@HL/NONOate group exhibited significant hair regrowth, with parameters such as skin color score (Figure S6a, b), total regenerated hair volume (Figure 5d), average hair weight (Figure 5e), hair coverage area (Figure 5f), and hair diameter (Figure S7a) closely matching those of the Healthy group. Further analysis using HE staining of skin tissue sections revealed that hair follicles in the Healthy and PVA@HL/NONOate groups were mature, while most follicles in the AGA group were in the telogen or catagen phases (Figure S7a). The Healthy group had the highest total number of hair follicles, closely followed by the PVA@HL/NONOate group, both significantly higher than the AGA group (Figure S6d).

To further explore the regulatory effects of NO on the hair follicle microenvironment at the tissue level, the changes in the levels of relevant inflammatory and proliferative factors around the hair follicles in each group of mice were measured after the completion of the experiments.[23] First, to verify that the injection of DHT could sustain the androgen-induced microenvironmental damage around hair follicles, we measured the androgen receptors (AR) levels in the mice from different groups.[24] As shown in Figure S8a, b, fluorescence quantification revealed that, compared to the Healthy group, the expression of AR was elevated to varying degrees in the other groups of mice. This indicates that the model can maintain hormone levels in mice over the long-term, closely resembling clinical conditions. Notably, the content of AR significantly decreased in mice treated with NO, suggesting that NO could inhibit the expression of AR around hair follicles, thereby reducing androgen levels. As depicted in Figure S9a, b, the levels of IL-6 and TGF-β1 were elevated in all groups compared to the Healthy group, with the NO-treated mice showing levels closest to the Healthy group. This indicates that low-concentration NO can effectively mitigate androgen-induced hair follicle damage through its anti-inflammatory effects. Additionally, mice in the Minoxidil group exhibited some hypersensitivity, leading to an increase in related indicators, highlighting the unavoidable side effects of minoxidil. After confirming the anti-inflammatory effects of low-concentration NO at both the cellular and tissue levels, we further assessed the ability of NO to promote the repair of the damaged hair follicle microenvironment by measuring two protein markers, Ki67 and VEGF, which are known to reflect tissue repair processes.[25] As illustrated in Figure S8a, c, d, the fluorescence quantification results showed significant expression of proliferation factors in the hair follicles after NO treatment, effectively repairing the hormone-induced damage to the hair follicle microenvironment, bringing it to a level comparable to that of the Healthy group. Thus, through various evaluative methods, we demonstrated that PVA@HL/NONOate can effectively suppress inflammation in the skin and hair follicles at the tissue level, promote angiogenesis in hair follicles, improve the hair growth microenvironment, and utilize NO to effectively treat AGA.

As shown in Figure S7b, the skin of the mice in the Minoxidil group developed flaking, while no abnormalities were observed on the skin surface of the other groups. Furthermore, H&E staining was performed on the major organs of mice after NO treatment. As shown in Figure S10a, no toxic reactions were observed in the tissues of any group. The evaluation of liver and kidney functions is of significant importance in assessing the therapeutic efficacy and safety of biomedical materials.[26] Based on the results shown in Figure S10b, we observed no significant differences in the liver and kidney function-related indicators between the treated mice and the Healthy group, with all indicators remaining within the standard requirements. To evaluate the hemocompatibility of PVA@HL/NONOate, fresh rabbit blood diluted with deionized water was used as the positive control, and PBS (pH = 7.4) was used as the negative control. The hemolysis rates of PVA@HL/NONOate at various concentrations were tested. As shown in Figure S11, the supernatants from the PVA@HL/NONOate group were similar to those of the PBS group, with hemolysis rates below 5%, significantly lower than that of the positive control. These results indicate that PVA@HL/NONOate exhibits good hemocompatibility. This finding further corroborates the biosafety of NO treatment, providing an excellent carrier for clinical gas therapy.

In this study, we successfully created a multistage transdermal nitric oxide (NO) delivery system PVA@HL/NONOate for the treatment of AGA. Cell experiments demonstrated that low-concentration NO could effectively enhance the cellular viability of HDPCs and HUVECs. High-throughput sequencing technology further proved that low-concentration NO could effectively treat AGA mainly by regulating HIF-1 signaling pathway to promote angiogenesis, reducing inflammation by downregulating the expression of TNFRSF9 and IL-6, repairing damaged hair follicles by downregulating the expression of genes in the CXCL5-IL-17 inflammatory axis. HA liposomes served as the primary

https://doi.org/10.1021/acsmaterialslett.4c01891
ACS Materials Lett. 2024, 6, 5354−5362

delivery vehicle, embedding the active NO molecules with a high loading capacity and extended release period. The PVA film with good mechanical flexibility as the secondary delivery carrier effectively prevented NO leakage, and enhanced the permeation and sustained release of NO in the skin, thus improving NO bioavailability. Furthermore, this transdermal delivery system also improved the inflammatory environment and upregulated the expression of proliferation proteins, achieving effective treatment of AGA in mice while demonstrating good biocompatibility. Thus, this study innovatively discovered the potential of NO in the treatment of AGA and provided a safer and more effective strategy for enhancing the effectiveness of gas transdermal therapy, offering significant applicability in the biomedical field.

■ ASSOCIATED CONTENT

Supporting Information

The Supporting Information is available free of charge at https://pubs.acs.org/doi/10.1021/acsmaterialslett.4c01891.

Additional experimental materials, methods, and characterization data for the preparation of multistage transdermal nitric oxide delivery system, other *in vitro* and *in vivo* experimental results, etc. (PDF)

■ AUTHOR INFORMATION

Corresponding Authors

Shixin Liu − *Guangdong Provincial Key Laboratory of Spine and Spinal Cord Reconstruction, The Fifth Affiliated Hospital (Heyuan Shenhe People's Hospital), Jinan University, Heyuan 517000, China*; Email: liushixin@jnu.edu.cn

Dong Ma − *Guangdong Provincial Key Laboratory of Spine and Spinal Cord Reconstruction, The Fifth Affiliated Hospital (Heyuan Shenhe People's Hospital), Jinan University, Heyuan 517000, China; Key Laboratory of Biomaterials of Guangdong Higher Education Institutes, Department of Biomedical Engineering, Jinan University, Guangzhou 510632, China*; orcid.org/0000-0002-1814-7348; Email: tmadong@jnu.edu.cn

Authors

Hui Xing − *Guangdong Provincial Key Laboratory of Spine and Spinal Cord Reconstruction, The Fifth Affiliated Hospital (Heyuan Shenhe People's Hospital), Jinan University, Heyuan 517000, China; Key Laboratory of Biomaterials of Guangdong Higher Education Institutes, Department of Biomedical Engineering, Jinan University, Guangzhou 510632, China*

Xinlin Jiang − *Guangdong Provincial Key Laboratory of Spine and Spinal Cord Reconstruction, The Fifth Affiliated Hospital (Heyuan Shenhe People's Hospital), Jinan University, Heyuan 517000, China; Key Laboratory of Biomaterials of Guangdong Higher Education Institutes, Department of Biomedical Engineering, Jinan University, Guangzhou 510632, China*

Ziyi Zhao − *Key Laboratory of Biomaterials of Guangdong Higher Education Institutes, Department of Biomedical Engineering, Jinan University, Guangzhou 510632, China*

Yuhui Yang − *Key Laboratory of Biomaterials of Guangdong Higher Education Institutes, Department of Biomedical Engineering, Jinan University, Guangzhou 510632, China*

Zhen Wang − *Key Laboratory of Biomaterials of Guangdong Higher Education Institutes, Department of Biomedical Engineering, Jinan University, Guangzhou 510632, China*

Yang Yi − *Key Laboratory of Biomaterials of Guangdong Higher Education Institutes, Department of Biomedical Engineering, Jinan University, Guangzhou 510632, China*

Guodong Sun − *Guangdong Provincial Key Laboratory of Spine and Spinal Cord Reconstruction, The Fifth Affiliated Hospital (Heyuan Shenhe People's Hospital), Jinan University, Heyuan 517000, China*

Complete contact information is available at: https://pubs.acs.org/10.1021/acsmaterialslett.4c01891

Author Contributions

[#]H.X. and X.J. contributed equally to this work. S.L. and D.M. designed the work. X.J. and H.X. wrote the manuscript. H.X. and Z.Z. performed the experiments and collected the data. Y.Y., Z.W., and Y.Y. helped with some measurements. H.X., G.S., and Z.W. analyzed the data. D.M. and S.L. provided research funding. All authors have given approval to the final version of the manuscript. CRediT: **Hui Xing** data curation, formal analysis, writing - original draft, writing - review & editing; **Xinlin Jiang** investigation, methodology, writing - original draft, writing - review & editing; **Ziyi Zhao** data curation, formal analysis; **Yuhui Yang** data curation, formal analysis; **Zhen Wang** formal analysis; **Yang Yi** data curation; **Guodong Sun** investigation; **Shixin Liu** funding acquisition, resources, writing - original draft, writing - review & editing; **Dong Ma** conceptualization, formal analysis, funding acquisition, methodology.

Notes

The authors declare no competing financial interest.

■ ACKNOWLEDGMENTS

This work was financially supported by the National Natural Science Foundation of China (32171369), the China Postdoctoral Science Foundation (2024M751133), and the Fundamental Research Funds for the Central Universities (11623410).

■ REFERENCES

(1) Gentile, P.; Garcovich, S. Systematic review of platelet-rich plasma use in androgenetic alopecia compared with Minoxidil®, Finasteride®, and adult stem cell-based therapy. *Int. J. Mol. Sci.* **2020**, *21*, 2702.

(2) Han, J. H.; Kwon, O. S.; Chung, J. H.; Cho, K. H.; Eun, H. C.; Kim, K. H. Effect of minoxidil on proliferation and apoptosis in dermal papilla cells of human hair follicle. *J. Dermatol Sci.* **2004**, *34*, 91−98.

(3) Yu, L.; Hu, P.; Chen, Y. Gas-generating nanoplatforms: material chemistry, multifunctionality, and gas therapy. *Adv. Mater.* **2018**, *30*, No. 1801964.

(4) Andrabi, S. M.; Sharma, N. S.; Karan, A.; Shahriar, S. S.; Cordon, B.; Ma, B.; Xie, J. Nitric oxide: physiological functions, delivery, and Biomedical Applications. *Adv. Sci.* **2023**, *10*, No. 2303259.

(5) Guo, Y.; Jing, D.; Liu, S.; Yuan, Q. Construction of intelligent moving micro/nanomotors and their applications in biosensing and disease treatment. *Theranostics.* **2023**, *13*, 2993.

(6) Xing, H.; Peng, H.; Yang, Y.; Lv, K.; Zhou, S.; Pan, X.; Wang, J.; Hu, Y.; Li, G.; Ma, D. Nitric oxide synergizes minoxidil delivered by transdermal hyaluronic acid liposomes for multimodal androgenetic-alopecia therapy. *Bioact Mater.* **2024**, *32*, 190−205.

(7) Yoshikawa, T.; Mori, Y.; Feng, H.; Phan, K. Q.; Kishimura, A.; Kang, J.-H.; Mori, T.; Katayama, Y. Rapid and continuous

accumulation of nitric oxide-releasing liposomes in tumors to augment the enhanced permeability and retention (EPR) effect. *Int. J. Pharm.* **2019**, *565*, 481−487.
(8) Jung, H. S.; Kim, K. S.; Yun, S. H.; Hahn, S. K. Enhancing the transdermal penetration of nanoconstructs: could hyaluronic acid be the key? *Nanomedicine.* **2014**, *9*, 743−745.
(9) Ni, C.; Zhang, Z.; Wang, Y.; Zhang, Z.; Guo, X.; Lv, H. Hyaluronic acid and HA-modified cationic liposomes for promoting skin penetration and retention. *J. Controlled Release* **2023**, *357*, 432−443.
(10) Paradossi, G.; Cavalieri, F.; Chiessi, E.; Spagnoli, C.; Cowman, M. K. Poly (vinyl alcohol) as versatile biomaterial for potential biomedical applications. *J. Mater. Sci. Mater. Med.* **2003**, *14*, 687−691.
(11) Ni, Y.; Zhao, W.; Cheng, W.; Deng, C.; Ying, Z.; Li, L.; Wang, X.; Sun, C.; Tu, J.; Jiang, L. Lipopeptide liposomes-loaded hydrogel for multistage transdermal chemotherapy of melanoma. *J. Controlled Release* **2022**, *351*, 245−254.
(12) Xie, J.; Ji, Y.; Xue, W.; Ma, D.; Hu, Y. Hyaluronic acid-containing ethosomes as a potential carrier for transdermal drug delivery. *Colloids Surf. B Biointerfaces* **2018**, *172*, 323−329.
(13) Pierre, M. B. R.; dos Santos Miranda Costa, I. Liposomal systems as drug delivery vehicles for dermal and transdermal applications. *Arch Dermatol Res.* **2011**, *303*, 607−621.
(14) Danaei, M.; Dehghankhold, M.; Ataei, S.; Hasanzadeh Davarani, F.; Javanmard, R.; Dokhani, A.; Khorasani, S.; Mozafari, M. Impact of particle size and polydispersity index on the clinical applications of lipidic nanocarrier systems. *Pharmaceutics.* **2018**, *10*, 57.
(15) Deng, Z.; Chen, M.; Liu, F.; Wang, Y.; Xu, S.; Sha, K.; Peng, Q.; Wu, Z.; Xiao, W.; Liu, T.; et al. Androgen receptor−mediated paracrine signaling induces regression of blood vessels in the dermal papilla in androgenetic alopecia. *J. Invest Dermatol.* **2022**, *142*, 2088−2099.e9.
(16) Otberg, N.; Finner, A. M.; Shapiro, J. Androgenetic alopecia. *Endocrinol Metab Clin North Am.* **2007**, *36*, 379−398.
(17) Oro, A. E.; Higgins, K. Hair cycle regulation of Hedgehog signal reception. *Dev. Biol.* **2003**, *255*, 238−248.
(18) Kim, Y. E.; Choi, H. C.; Lee, I.-C.; Yuk, D. Y.; Lee, H.; Choi, B. Y. 3-Deoxysappanchalcone promotes proliferation of human hair follicle dermal papilla cells and hair growth in C57BL/6 mice by modulating WNT/β-Catenin and STAT signaling. *Biomol Ther.* **2016**, *24*, 572.
(19) Ansó, E.; Zuazo, A.; Irigoyen, M.; Urdaci, M. C.; Rouzaut, A.; Martínez-Irujo, J. J. Flavonoids inhibit hypoxia-induced vascular endothelial growth factor expression by a HIF-1 independent mechanism. *Biochem. Pharmacol.* **2010**, *79*, 1600−1609.
(20) Mathur, A. N.; Zirak, B.; Boothby, I. C.; Tan, M.; Cohen, J. N.; Mauro, T. M.; Mehta, P.; Lowe, M. M.; Abbas, A. K.; Ali, N.; et al. Treg-cell control of a CXCL5-IL-17 inflammatory axis promotes hair-follicle-stem-cell differentiation during skin-barrier repair. *Immunity* **2019**, *50*, 655−667. e4.
(21) Mokabber, H.; Vatankhah, M. A.; Najafzadeh, N. The regulatory role of microRNAs in the development, cyclic changes, and cell differentiation of the hair follicle. *Process Biochem.* **2022**, *114*, 36−41.
(22) Han, S.; Chi, Y.; Yang, Z.; Ma, J.; Wang, L. Tumor Microenvironment Regulation and Cancer Targeting Therapy Based on Nanoparticles. *J. Funct Biomater.* **2023**, *14*, 136.
(23) Guan, Q.; Guo, Z.-h.; Dai, D.-m.; Fan, Z.-x.; Chen, J.; Wu, S.-l.; Liu, X.-m.; Miao, Y.; Hu, Z.-q.; Qu, Q. Platelet lysate promotes hair growth: *In vitro* and *in vivo* mechanism and randomized, controlled trial. *Biomed Pharmacother* **2023**, *161*, No. 114517.
(24) Ji, S.; Zhu, Z.; Sun, X.; Fu, X. Functional hair follicle regeneration: an updated review. *Sig. Transduct. Target. Ther.* **2021**, *6*, 66.
(25) Elsebay, S. A. G.; Nada, H. F.; Sultan, N. S. S.; El-Waseef, D. A. E.-D. A. Comparative histological and immunohistochemical study on the effect of platelet rich plasma/minoxidil, alone or in combination, on hair growth in a rat model of androgenic alopecia. *Tissue Cell.* **2022**, *75*, No. 101726.
(26) Wang, W.; Zhou, S.; Cheng, Z.; Ma, D.; Liu, T. A glutathione-sensitive cationic polymer delivery of CRISPR-Cas9 RNA plasmid for targeting nasopharyngeal carcinoma gene therapy. *Colloids Surf. B Biointerfaces* **2023**, *223*, No. 113146.

https://doi.org/10.1021/acsmaterialslett.4c01891
ACS Materials Lett. 2024, 6, 5354−5362